

A NEW MATHEMATICAL MODEL FOR DESIGN OF SQUARE ISOLATED FOOTINGS FOR GENERAL CASE

SANDRA LÓPEZ CHAVARRÍA, ARNULFO LUÉVANOS ROJAS
AND MANUEL MEDINA ELIZONDO

Instituto de Investigaciones Multidisciplinaria
Facultad de Contaduría y Administración
Universidad Autónoma de Coahuila
Blvd. Revolución 151 Ote. CP 27000, Torreón, Coahuila, México
arnulfol_2007@hotmail.com

Received January 2017; revised May 2017

ABSTRACT. *This paper presents a new mathematical model for design of square isolated footings for the general case, i.e., the column subjected to an axial load and moments in two directions in the joint with the footing, and the column is localized anywhere of the footing. The main part of this research is that the new model considers the soil real pressure and it is presented in terms of the mechanical elements (P , M_x and M_y), and the classical model takes account of the maximum pressure and it is considered uniform at all the contact area of the footing. The new model is verified by balance of forces and moments in the main points of the footing. Also a comparison is presented between the new model and the classical model by three examples, and the results show that the classical model is bigger in terms of design with respect to the new model. Then, the new model is the most appropriate, since it is adjusted to the real conditions of the soil, and the forces and moments comply with balance condition, and also is more economic.*

Keywords: Square isolated footings, Mathematical models, Contact surface, Moments, Bending shear, Punching shear

1. Introduction. The purpose of the foundation is to effectively support the superstructure by transmitting the applied load effects (forces and moments) to the soil below, without exceeding the bearing capacity of the soil, and ensuring that the settlements of the structure are within tolerable limits, and as nearly uniform as possible [1,2].

The foundations are classified as shallow and deep, which have important differences: in terms of geometry, the behavior of the soil, its structural functionality and its constructive systems [1,2]. Shallow foundations are provided when the ratio of $H/B < 1$, where H is the depth of footing and B is the width of footing. Deep foundations are provided when the ratio of $H/B \geq 1$. Shallow foundations may be of various types according to their function: isolated footing, combined footing, strip footing, or mat foundation [1-6]. The isolated footings can have different shapes in plan. Generally it depends on the shape of column cross section, and some of the popular shapes of footings are: square, rectangular and circular [7-9].

Footings belong to the category of shallow foundations (as opposed to deep foundations such as piles and caissons) and are used when soil has a sufficient strength to a small depth below the ground surface. Shallow foundations (footings) have a large plan area in comparison with the cross-sectional area of the column.

The design of shallow foundations in terms of the application of loads is: 1) the footings subjected to an axial load, 2) the footings subjected to an axial load and moment in one

direction (uniaxial bending), 3) the footings subjected to an axial load and moment in two directions (biaxial bending) [1-6].

The distribution of soil pressure under a footing is a function of the type of soil, the relative rigidity of the soil and the footing, and the depth of foundation at level of contact between footing and soil. A concrete footing on sand will have a pressure distribution similar to Figure 1(a). When a rigid footing is resting on sandy soil, the sand near the edges of the footing tends to displace laterally when the footing is loaded. This tends to decrease in soil pressure near the edges, whereas soil away from the edges of footing is relatively confined. On the other hand, the pressure distribution under a footing on clay is similar to Figure 1(b). As the footing is loaded, the soil under the footing deflects in a bowl-shaped depression, relieving the pressure under the middle of the footing. For design purposes, it is common to assume the soil pressures are linearly distributed. The pressure distribution will be uniform if the centroid of the footing coincides with the resultant of the applied loads, as shown in Figure 1(c) [1].

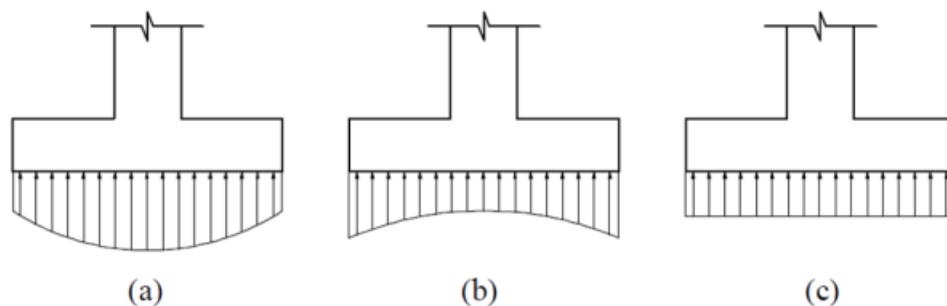


FIGURE 1. Pressure distribution under footing: (a) footing on sand; (b) footing on clay; (c) equivalent uniform distribution

The hypothesis used in the classical model is to consider the uniform pressure for the design, i.e., the same pressure at all points of contact in the foundation with the soil; this design pressure is the maximum value that occurs in an isolated footing [1-6].

The most relevant papers addressing the issue of the foundations models are: Yin realized a comparative modeling study of reinforced beam on elastic foundation between the finite element model (FEM) and the Timoshenko beam model (TBM) [10]; Smith-Pardo presented nonlinear time-history analyses of wall-frame structural models indicate that the condition of vulnerable foundations for which uplifting and reaching the bearing capacity of the supporting soil can occur before yielding at the base of the shear walls may not be necessarily detrimental to the drift response of buildings under strong ground motions [11]; Agrawal and Hora made a study on the nonlinear interaction behaviour of infilled frame-isolated footings-soil system subjected to seismic loading [12]; Maheshwari and Khatri presented the influence of inclusion of geosynthetic layer on response of combined footings on stone column reinforced earth beds [13]; Luévanos Rojas et al. proposed a design of isolated footings of rectangular form using a new model and the column is located in the center of the footing [14]; Dixit and Patil estimated experimentally the values of $N\gamma$ (bearing capacity factor) and corresponding settlements for square footings on finite layer of sand [15]; Cure et al. developed a series of bearing capacity tests was conducted with eccentrically loaded model surface and shallow strip footings resting close to a slope to investigate behavior of such footings (ultimate loads, failure surfaces, load-displacement curves, rotation of footing, etc.) [16]; Luévanos Rojas has presented several studies on footings, which are: design of isolated footings of circular form using a new model and the column is located in the center of the footing [17]; design

of boundary combined footings of rectangular shape using a new model, in this paper one column is located in the property line of the construction and the other column is located on the interior part of the construction aligned with the edge column located in direction perpendicular to the property line [18]; design of boundary combined footings of trapezoidal form using a new model, in this paper it presents the same situation as the previous paper but the footing is trapezoidal [19]; a comparative study for the design of rectangular and circular isolated footings using new models and the column is located in the center of each footing for the two models [20]; a new model for design of boundary rectangular combined footings with two opposite sides constrained, and in this paper the two columns are located in the property lines of opposite sides [21].

This paper presents in its theoretical part a new mathematical model for design of square isolated footings for the general case, i.e., the column subjected to an axial load and moments in two directions in the joint with the footing, and the column is localized anywhere of the footing. The main part of this research is that new model considers the real pressure of the soil, this is presented in terms of the mechanical elements (P , M_x and M_y) and the classical model takes account of the maximum pressure and it is considered uniform at all the contact area of the footing.

The paper is organized as follows. Section 2 describes the formulation of the new mathematical model for design of square isolated footings for the general case, and the equations for moments, bending shear and punching shear are shown. Section 3 shows the classical model. The validation of the new mathematical model is presented in Section 4. Section 5 shows three numerical examples for design of square isolated footings supporting one square column and the dimensions are obtained using optimization techniques, and the three examples are: concentric footing, edge footing and corner footing. Results and discussion are presented in Section 6. Conclusions (Section 7) complete the paper.

2. Formulation of the New Mathematical Model. According to Building Code Requirements for Structural Concrete and Commentary, the critical sections are: 1) the maximum moment is located in face of column, pedestal, or wall, for footings supporting a concrete column, pedestal, or wall; 2) bending shear presented at a distance “ d ” (distance from extreme compression fiber to centroid of longitudinal tension reinforcement) shall be measured from face of column, pedestal, or wall for footings supporting a column, pedestal, or wall; 3) punching shear is localized so that its perimeter “ b_o ” is a minimum but need not approach closer than “ $d/2$ ” to: (a) edges or corners of columns, concentrated loads, or reaction areas, and (b) changes in slab thickness such as edges of capitals, drop panels, or shear caps [22].

Figure 2 shows a square footing subjected to an axial load and moment in two directions (biaxial bending) and the column is localized anywhere of the footing, where pressure is different in the four corners of the contact surface [23].

The general equation for any type of footings subjected to biaxial bending is [1-4,14,17-21,23,24]:

$$\sigma = \frac{P}{A} \pm \frac{M_{xT}y}{I_x} \pm \frac{M_{yT}x}{I_y} \quad (1)$$

where σ is the pressure exerted by the soil on the footing, A is the contact area of the footing, P is the axial load applied at the center of gravity of the footing, M_{xT} is the total moment around the axis “ X ”, M_{yT} is the total moment around the axis “ Y ”, x is the distance in the direction “ X ” measured from the axis “ Y ” up the fiber under study, y is the distance in direction “ Y ” measured from the axis “ X ” up the fiber under study, I_y is the moment of inertia around the axis “ Y ” and I_x is the moment of inertia around the axis “ X ”.

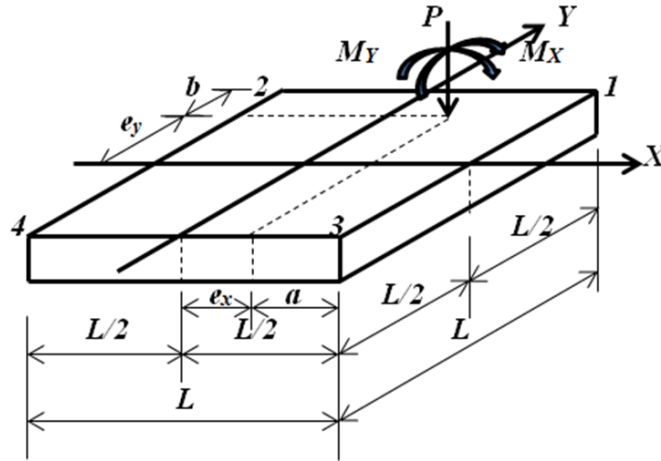


FIGURE 2. Square footing under a column localized anywhere of the footing

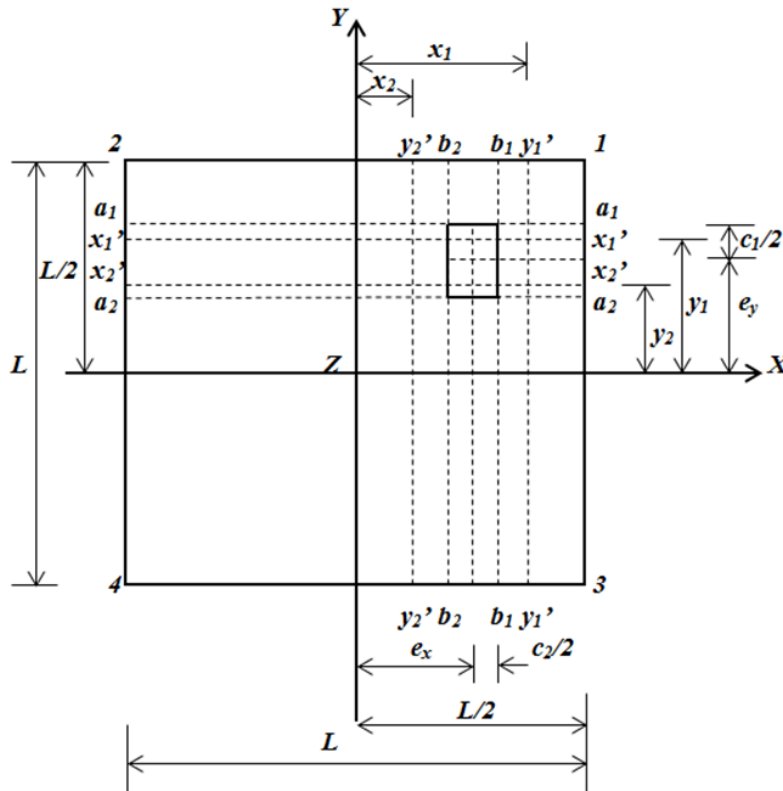


FIGURE 3. Critical sections for moments

Substitute $M_{xT} = M_x + Pe_y$, $M_{yT} = M_y + Pe_x$, $A = L^2$, $I_x = I_y = L^4/12$ into Equation (1) and the pressure exerted by the soil anywhere on the footing in function of coordinates (x, y) is obtained [23]:

$$\sigma(x, y) = \frac{P}{L^2} + \frac{12(M_x + Pe_y)y}{L^4} + \frac{12(M_y + Pe_x)x}{L^4} \tag{2}$$

2.1. **Moments.** Critical sections for moments are presented in section a_1 - a_1 , a_2 - a_2 , b_1 - b_1 and b_2 - b_2 , as shown in Figure 3.

2.1.1. *Moment around the axis “ x'_1 - x'_1 ” for “ $e_y \leq y_1 \leq L/2$ ”.* Shear force “ V_{y_1} ” is obtained by means of the pressure volume of the area formed by the axis x'_1 - x'_1 and the corners 1

and 2 of the footing:

$$V_{y_1} = - \int_{y_1}^{L/2} \int_{-L/2}^{L/2} \sigma(x, y) dx dy \tag{3}$$

$$V_{y_1} = -\frac{P}{2} - \frac{3(M_x + Pe_y)}{2L} + \frac{Py_1}{L} + \frac{6(M_x + Pe_y)y_1^2}{L^3} \tag{4}$$

If the derivation of the moment is the shear force, it is presented as follows:

$$V_{y_1} = \frac{dM_{x'_1}}{dy_1} \tag{5}$$

where $M_{x'_1}$ is the moment around the axis “ x'_1 ” and V_{y_1} is the shear force at a distance “ y_1 ”.

Then, the moment is:

$$M_{x'_1} = \int \left(-\frac{P}{2} - \frac{3(M_x + Pe_y)}{2L} + \frac{Py_1}{L} + \frac{6(M_x + Pe_y)y_1^2}{L^3} \right) dy_1 \tag{6}$$

$$M_{x'_1} = -\frac{Py_1}{2} - \frac{3(M_x + Pe_y)y_1}{2L} + \frac{Py_1^2}{2L} + \frac{2(M_x + Pe_y)y_1^3}{L^3} + C_1 \tag{7}$$

Substituting “ $y_1 = L/2$ ” and $M_{x'_1} = 0$ into Equation (7), the constant “ C_1 ” is obtained:

$$C_1 = \frac{PL}{8} + \frac{(M_x + Pe_y)}{2} \tag{8}$$

Now, substituting Equation (8) into Equation (7) to find the moments equation, this is:

$$M_{x'_1} = \frac{P(L - 2y_1)^2}{8L} + \frac{(M_x + Pe_y)(4y_1^3 - 3L^2y_1 + L^3)}{2L^3} \tag{9}$$

Substituting “ $y_1 = c_1/2 + e_y$ ” into Equation (9) to obtain M_{a_1} (moment around the axis “ a_1-a_1 ”), this is:

$$M_{a_1} = \frac{P(L - c_1 - 2e_y)^2}{8L} + \frac{(M_x + Pe_y)[4(c_1/2 + e_y)^3 - 3L^2(c_1/2 + e_y) + L^3]}{2L^3} \tag{10}$$

Substituting “ $y_1 = e_y$ ” into Equation (9) to find $M_{c_1/2}$ (moment around the axis located in the column center), this is:

$$M_{c_1/2} = \frac{P(L - 2e_y)^2}{8L} + \frac{(M_x + Pe_y)(4e_y^3 - 3L^2e_y + L^3)}{2L^3} \tag{11}$$

2.1.2. *Moment around the axis “ $x'_2-x'_2$ ” for “ $-L/2 \leq y_2 \leq e_y$ ”.* Shear force “ V_{y_2} ” is found by means of the pressure volume of the area formed by the axis $x'_2-x'_2$ and the corners 1 and 2 of the footing:

$$V_{y_2} = P - \int_{y_2}^{L/2} \int_{-L/2}^{L/2} \sigma(x, y) dx dy \tag{12}$$

$$V_{y_2} = \frac{P}{2} - \frac{3(M_x + Pe_y)}{2L} + \frac{Py_2}{L} + \frac{6(M_x + Pe_y)y_2^2}{L^3} \tag{13}$$

If the derivation of the moment is the shear force, it is presented as follows:

$$V_{y_2} = \frac{dM_{x'_2}}{dy_2} \tag{14}$$

where $M_{x'_2}$ is the moment around the axis “ x'_2 ” and V_{y_2} is the shear force at a distance “ y_2 ”.

Then, the moment is:

$$M_{x'_2} = \int \left(\frac{P}{2} - \frac{3(M_x + Pe_y)}{2L} + \frac{Py_2}{L} + \frac{6(M_x + Pe_y)y_2^2}{L^3} \right) dy_2 \tag{15}$$

$$M_{x'_2} = \frac{Py_2}{2} - \frac{3(M_x + Pe_y)y_2}{2L} + \frac{Py_2^2}{2L} + \frac{2(M_x + Pe_y)y_2^3}{L^3} + C_2 \tag{16}$$

Substituting “ $y_2 = e_y$ ”, $M_{c_1/2} = \frac{P(L-2e_y)^2}{8L} + \frac{(M_x+Pe_y)(4e_y^3-3L^2e_y+L^3)}{2L^3} - M_x$ into Equation (16), the constant “ C_2 ” is obtained:

$$C_2 = \frac{PL}{8} - \frac{(M_x + Pe_y)}{2} \tag{17}$$

Now, substituting Equation (17) into Equation (16) to find the moments equation, this is:

$$M_{x'_2} = \frac{P(L + 2y_2)^2}{8L} + \frac{(M_x + Pe_y)(4y_2^3 - 3L^2y_2 - L^3)}{2L^3} \tag{18}$$

Substituting “ $y_2 = e_y - c_1/2$ ” into Equation (18) to obtain M_{a_2} (moment around the axis “ a_2-a_2 ”), this is:

$$M_{a_2} = \frac{P(L + 2e_y - c_1)^2}{8L} + \frac{(M_x + Pe_y)[4(e_y - c_1/2)^3 - 3L^2(e_y - c_1/2) - L^3]}{2L^3} \tag{19}$$

2.1.3. *Moment around the axis “ $y'_1-y'_1$ ” for “ $e_x \leq x_1 \leq L/2$ ”.* Shear force “ V_{x_1} ” is obtained by means of the pressure volume of the area formed by the axis $y'_1-y'_1$ and the corners 1 and 3 of the footing:

$$V_{x_1} = - \int_{-L/2}^{L/2} \int_{x_1}^{L/2} \sigma(x, y) dx dy \tag{20}$$

$$V_{x_1} = -\frac{P}{2} - \frac{3(M_y + Pe_x)}{2L} + \frac{Px_1}{L} + \frac{6(M_y + Pe_x)x_1^2}{L^3} \tag{21}$$

If the derivation of the moment is the shear force, it is presented as follows:

$$V_{x_1} = \frac{dM_{y'_1}}{dx_1} \tag{22}$$

where $M_{y'_1}$ is the moment around the axis “ y'_1 ” and V_{x_1} is the shear force at a distance “ x_1 ”.

Then, the moment is:

$$M_{y'_1} = \int \left(-\frac{P}{2} - \frac{3(M_y + Pe_x)}{2L} + \frac{Px_1}{L} + \frac{6(M_y + Pe_x)x_1^2}{L^3} \right) dx_1 \tag{23}$$

$$M_{y'_1} = -\frac{Px_1}{2} - \frac{3(M_y + Pe_x)x_1}{2L} + \frac{Px_1^2}{2L} + \frac{6(M_y + Pe_x)x_1^3}{3L^3} + C_3 \tag{24}$$

Substituting “ $x_1 = L/2$ ” and $M_{y'_1} = 0$ into Equation (24), the constant “ C_3 ” is obtained:

$$C_3 = \frac{PL}{8} + \frac{(M_y + Pe_x)}{2} \tag{25}$$

Now, substituting Equation (25) into Equation (24) to find the moments equation, this is:

$$M_{y'_1} = \frac{P(L - 2x_1)^2}{8L} + \frac{(M_y + Pe_x)(4x_1^3 - 3L^2x_1 + L^3)}{2L^3} \tag{26}$$

Substituting “ $x_1 = c_2/2 + e_x$ ” into Equation (26) to obtain M_{b_1} (moment around the axis “ b_1-b_1 ”), this is:

$$M_{b_1} = \frac{P(L - c_2 - 2e_x)^2}{8L} + \frac{(M_y + Pe_x)[4(c_2/2 + e_x)^3 - 3L^2(c_2/2 + e_x) + L^3]}{2L^3} \tag{27}$$

Substituting “ $x_1 = e_x$ ” into Equation (26) to find $M_{c_2/2}$ (moment around the axis located in the column center), this is:

$$M_{c_2/2} = \frac{P(L - 2e_x)^2}{8L} + \frac{(M_y + Pe_x)(4e_x^3 - 3L^2e_x + L^3)}{2L^3} \tag{28}$$

2.1.4. *Moment around the axis “ y'_2 - y'_2 ” for “ $-L/2 \leq x_2 \leq e_x$ ”.* Shear force “ V_{x_2} ” is found by means of the pressure volume of the area formed by the axis y'_2 - y'_2 and the corners 1 and 3 of the footing:

$$V_{x_2} = P - \int_{-L/2}^{L/2} \int_{x_2}^{L/2} \sigma(x, y) dx dy \tag{29}$$

$$V_{x_2} = \frac{P}{2} - \frac{3(M_y + Pe_x)}{2L} + \frac{Px_2}{L} + \frac{6(M_y + Pe_x)x_2^2}{L^3} \tag{30}$$

If the derivation of the moment is the shear force, it is presented as follows:

$$V_{x_2} = \frac{dM_{y'_2}}{dx_2} \tag{31}$$

where $M_{y'_2}$ is the moment around the axis “ y'_2 ” and V_{x_2} is the shear force at a distance “ x_2 ”.

Then, the moment is:

$$M_{y'_2} = \int \left(\frac{P}{2} - \frac{3(M_y + Pe_x)}{2L} + \frac{Px_2}{L} + \frac{6(M_y + Pe_x)x_2^2}{L^3} \right) dx_2 \tag{32}$$

$$M_{y'_2} = \frac{Px_2}{2} - \frac{3(M_y + Pe_x)x_2}{2L} + \frac{Px_2^2}{2L} + \frac{6(M_y + Pe_x)x_2^3}{3L^3} + C_4 \tag{33}$$

Substituting “ $x_2 = e_x$ ”, $M_{c_2/2} = \frac{P(L-2e_x)^2}{8L} + \frac{(M_y+Pe_x)(4e_x^3-3L^2e_x+L^3)}{2L^3} - M_y$ into Equation (33), the constant “ C_4 ” is obtained:

$$C_4 = \frac{PL}{8} - \frac{(M_y + Pe_x)}{2} \tag{34}$$

Now, substituting Equation (34) into Equation (33) to find the moments equation, this is:

$$M_{y'_2} = \frac{P(L + 2x_2)^2}{8L} + \frac{(M_y + Pe_x)(4x_2^3 - 3L^2x_2 - L^3)}{2L^3} \tag{35}$$

Substituting “ $x_2 = e_x - c_2/2$ ” into Equation (35) to obtain M_{b_2} (moment around the axis “ b_2 - b_2 ”), this is:

$$M_{b_2} = \frac{P(L + 2e_x - c_2)^2}{8L} + \frac{(M_y + Pe_x)[4(e_x - c_2/2)^3 - 3L^2(e_x - c_2/2) - L^3]}{2L^3} \tag{36}$$

2.2. Bending shear (unidirectional shear force). Critical sections for bending shear at a distance “ d ” starting the junction of the column with the footing as seen in Figure 4 are obtained, which are presented in sections f_1 - f_1 , f_2 - f_2 , g_1 - g_1 and g_2 - g_2 .

2.2.1. *Bending shear on axis f_1 - f_1 .* Substituting “ $y_1 = e_y + c_1/2 + d$ ” into Equation (4) to obtain the bending shear on the axis f_1 - f_1 of the footing “ V_{f_1} ” (area formed by the axis f_1 - f_1 and the corners 1 and 2), this is:

$$V_{f_1} = \frac{P(2e_y + c_1 + 2d - L)}{2L} + \frac{3(M_x + Pe_y)[4(e_y + c_1/2 + d)^2 - L^2]}{2L^3} \tag{37}$$

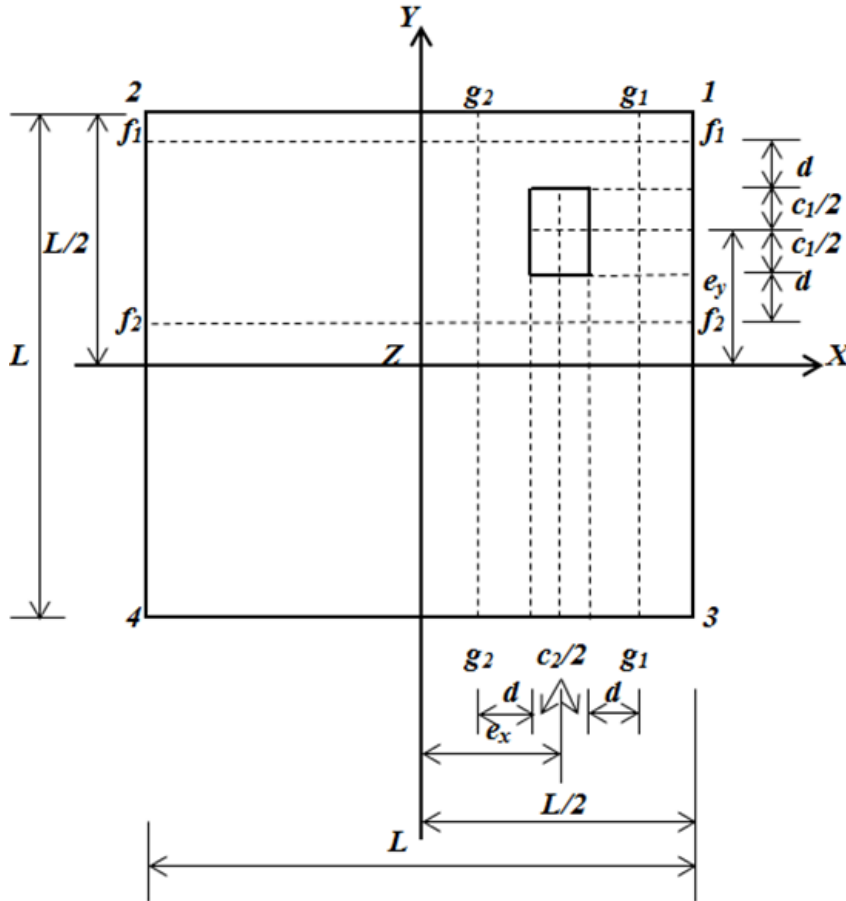


FIGURE 4. Critical sections for bending shear

2.2.2. *Bending shear on axis f_2 - f_2 .* Substituting “ $y_2 = e_y - c_1/2 - d$ ” into Equation (13) to obtain the bending shear on the axis f_2 - f_2 of the footing “ V_{f_2} ” (area formed by the axis f_2 - f_2 and the corners 1 and 2), this is:

$$V_{f_2} = \frac{P(L + 2e_y - c_1 - 2d)}{2L} + \frac{3(M_x + Pe_y) [4(e_y - c_1/2 - d)^2 - L^2]}{2L^3} \quad (38)$$

2.2.3. *Bending shear on axis g_1 - g_1 .* Substituting “ $x_1 = e_x + c_2/2 + d$ ” into Equation (21) to obtain the bending shear on the axis g_1 - g_1 of the footing “ V_{g_1} ” (area formed by the axis g_1 - g_1 and the corners 1 and 3), this is:

$$V_{g_1} = \frac{P(2e_x + c_2 + 2d - L)}{2L} + \frac{3(M_y + Pe_x) [4(e_x + c_2/2 + d)^2 - L^2]}{2L^3} \quad (39)$$

2.2.4. *Bending shear on axis g_2 - g_2 .* Substituting “ $x_2 = e_x - c_2/2 - d$ ” into Equation (30) to obtain the bending shear on the axis g_2 - g_2 of the footing “ V_{g_2} ” (area formed by the axis g_2 - g_2 and the corners 1 and 3), this is:

$$V_{g_2} = \frac{P(L + 2e_x - c_2 - 2d)}{2L} + \frac{3(M_y + Pe_x) [4(e_x - c_2/2 - d)^2 - L^2]}{2L^3} \quad (40)$$

2.3. **Punching shear (bidirectional shear force).** Critical section for the punching shear appears at a distance “ $d/2$ ” starting the junction of the column with the footing in the two directions, as shown in Figure 5.

Critical section for the punching shear occurs in rectangular section formed by points 5, 6, 7 and 8, as shown in Figure 5. Punching shear acting on the footing “ V_p ” is the force

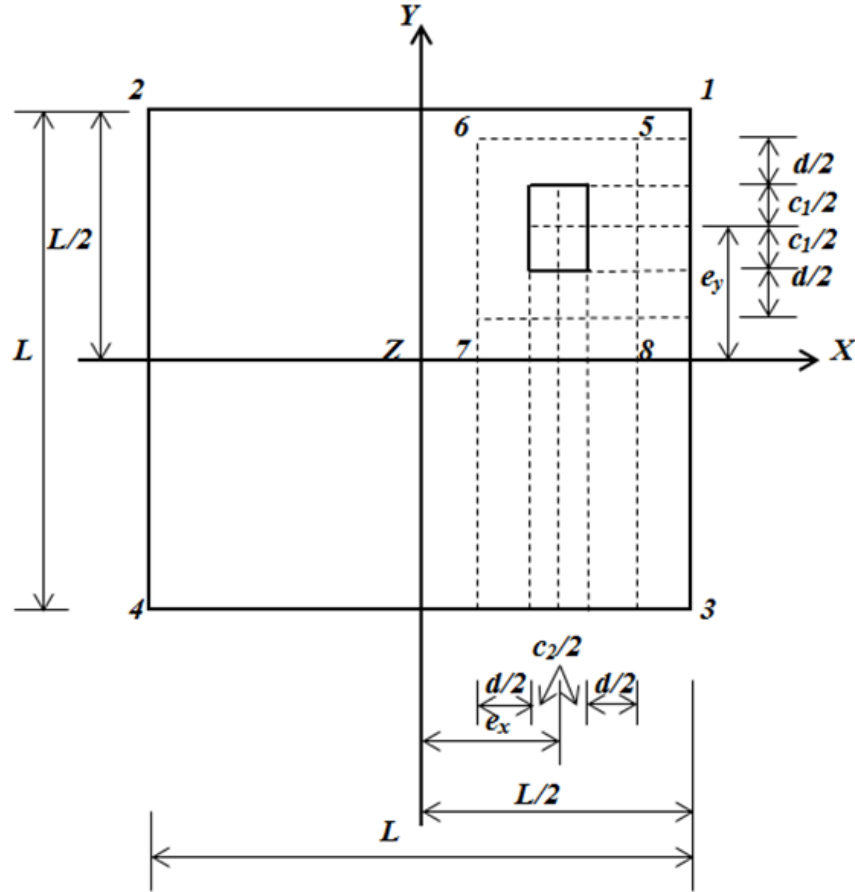


FIGURE 5. Critical sections for the punching shear

“ P ” acting on column subtracting the pressure volume of the area formed by the points 5, 6, 7 and 8.

2.3.1. *To general case.* Limits of the subtracted area are: Limits in direction “ Y ” are of $e_y + c_1/2 + d/2$ (points 5 and 6) to $e_y - c_1/2 - d/2$ (points 7 and 8). Limits in direction “ X ” are of $e_x + c_2/2 + d/2$ (points 5 and 8) to $e_x - c_2/2 - d/2$ (points 6 and 7). Then V_p is:

$$V_p = P - \int_{e_y - c_1/2 - d/2}^{e_y + c_1/2 + d/2} \int_{e_x - c_2/2 - d/2}^{e_x + c_2/2 + d/2} \sigma(x, y) dx dy \quad (41)$$

$$V_p = P - \frac{[PL^2 + 12e_y(M_x + Pe_y) + 12e_x(M_y + Pe_x)](c_1 + d)(c_2 + d)}{L^4} \quad (42)$$

Equation (42) satisfies for $e_y \leq L/2 - c_1/2 - d/2$ and $e_x \leq L/2 - c_2/2 - d/2$.

2.3.2. *To specific cases.*

To concentric footings: Limits of the subtracted area are: Limits in direction “ Y ” are of $c_1/2 + d/2$ (points 5 and 6) to $-c_1/2 - d/2$ (points 7 and 8). Limits in direction “ X ” are of $c_2/2 + d/2$ (points 5 and 8) to $-c_2/2 - d/2$ (points 6 and 7). Then V_p is:

$$V_p = P - \int_{-c_1/2 - d/2}^{c_1/2 + d/2} \int_{-c_2/2 - d/2}^{c_2/2 + d/2} \sigma(x, y) dx dy \quad (43)$$

$$V_p = P - \frac{P(c_1 + d)(c_2 + d)}{L^2} \quad (44)$$

To edge footings in end of the axis “X-X”: Limits of the subtracted area are: Limits in direction “Y” are of $c_1/2 + d/2$ (points 5 and 6) to $-c_1/2 - d/2$ (points 7 and 8). Limits in direction “X” are of $L/2$ (points 5 and 8) to $L/2 - c_2/2 - d/2$ (points 6 and 7). Then V_p is:

$$V_p = P - \int_{-c_1/2-d/2}^{c_1/2+d/2} \int_{L/2-c_2-d/2}^{L/2} \sigma(x, y) dx dy \tag{45}$$

$$V_p = P - \frac{P(c_1 + d)(2c_2 + d)}{2L^2} - \frac{3[2M_y + P(L - c_2)](L - c_2 - d/2)(c_1 + d)(2c_2 + d)}{2L^4} \tag{46}$$

To edge footings in end of the axis “Y-Y”: Limits of the subtracted area are: Limits in direction “Y” are of $L/2$ (points 5 and 6) to $L/2 - c_1/2 - d/2$ (points 7 and 8). Limits in direction “X” are of $c_2/2 + d/2$ (points 5 and 8) to $-c_2/2 - d/2$ (points 6 and 7). Then V_p is:

$$V_p = P - \int_{L/2-c_1-d/2}^{L/2} \int_{-c_2/2-d/2}^{c_2/2+d/2} \sigma(x, y) dx dy \tag{47}$$

$$V_p = P - \frac{P(c_2 + d)(2c_1 + d)}{2L^2} - \frac{3[2M_x + P(L - c_1)](L - c_1 - d/2)(c_2 + d)(2c_1 + d)}{2L^4} \tag{48}$$

To corner footings: Limits of the subtracted area are: Limits in direction “Y” are of $L/2$ (points 5 and 6) to $L/2 - c_1/2 - d/2$ (points 7 and 8). Limits in direction “X” are of $L/2$ (points 5 and 8) to $L/2 - c_2/2 - d/2$ (points 6 and 7). Then V_p is:

$$V_p = P - \int_{L/2-c_1-d/2}^{L/2} \int_{L/2-c_2-d/2}^{L/2} \sigma(x, y) dx dy \tag{49}$$

$$V_p = P - \frac{P(2c_1 + d)(2c_2 + d)}{4L^2} - \frac{3[2M_x + P(L - c_1)](L - c_1 - d/2)(2c_1 + d)(2c_2 + d)}{4L^4} - \frac{3[2M_y + P(L - c_2)](L - c_2 - d/2)(2c_1 + d)(2c_2 + d)}{4L^4} \tag{50}$$

3. Classical Model. The maximum pressure exerted by the soil in the four corners is obtained as follows:

$$\sigma_1 = \frac{P}{L^2} + \frac{6(M_x + Pe_y)}{L^3} + \frac{6(M_y + Pe_x)}{L^3} \tag{51}$$

$$\sigma_2 = \frac{P}{L^2} + \frac{6(M_x + Pe_y)}{L^3} - \frac{6(M_y + Pe_x)}{L^3} \tag{52}$$

$$\sigma_3 = \frac{P}{L^2} - \frac{6(M_x + Pe_y)}{L^3} + \frac{6(M_y + Pe_x)}{L^3} \tag{53}$$

$$\sigma_4 = \frac{P}{L^2} - \frac{6(M_x + Pe_y)}{L^3} - \frac{6(M_y + Pe_x)}{L^3} \tag{54}$$

where $\sigma_{\max} \geq \sigma_1, \sigma_2, \sigma_3, \sigma_4$.

3.1. Moments. Critical sections for moments are presented in sections a_1 - a_1 , a_2 - a_2 , b_1 - b_1 and b_2 - b_2 , as shown in Figure 3. The moment in each section is:

$$M_{a_1} = \frac{\sigma_{\max} L(L/2 - e_y - c_1/2)^2}{2} \tag{55}$$

$$M_{a_2} = \frac{\sigma_{\max} L(L/2 + e_y - c_1/2)^2}{2} \tag{56}$$

$$M_{b_1} = \frac{\sigma_{\max} L(L/2 - e_x - c_2/2)^2}{2} \tag{57}$$

$$M_{b2} = \frac{\sigma_{\max}L(L/2 + e_x - c_2/2)^2}{2} \tag{58}$$

3.2. Bending shear (unidirectional shear force). Critical sections for bending shear are shown in sections f_1-f_1 , f_2-f_2 , g_1-g_1 and g_2-g_2 , as presented in Figure 4. The bending shear in each section is:

$$V_{f_1} = \sigma_{\max}L(L/2 - e_y - c_1/2 - d) \tag{59}$$

$$V_{f_2} = \sigma_{\max}L(L/2 + e_y - c_1/2 - d) \tag{60}$$

$$V_{g_1} = \sigma_{\max}L(L/2 - e_x - c_2/2 - d) \tag{61}$$

$$V_{g_2} = \sigma_{\max}L(L/2 + e_x - c_2/2 - d) \tag{62}$$

3.3. Punching shear (bidirectional shear force). Critical sections for punching shear are presented in Figure 5.

To concentric footings:

$$V_p = \sigma_{\max} [L^2 - (c_1 + d)(c_2 + d)] \tag{63}$$

To edge footings in end of the axis “X-X” is:

$$V_p = \sigma_{\max} [L^2 - (c_1 + d)(c_2 + d/2)] \tag{64}$$

To edge footings in end of the axis “Y-Y” is:

$$V_p = \sigma_{\max} [L^2 - (c_1 + d/2)(c_2 + d)] \tag{65}$$

To corner footings:

$$V_p = \sigma_{\max} [L^2 - (c_1 + d/2)(c_2 + d/2)] \tag{66}$$

4. Validation of the New Mathematical Model. Effects that govern the design for isolated footings are the moments, bending shear, and punching shear.

One way to validate the model is as follows.

- To moments
 - a) If the axis “ $x'_1-x'_1$ ” at the free end of the footing is located, then $y_1 = L/2$ is substituted into Equation (9) and the moment is $M = 0$.
 - b) If the axis “ $x'_1-x'_1$ ” in the center of the column is located, $y_1 = e_y$ is substituted into Equation (9) and the moment is $M_{c_1/2} = \frac{P(L-2e_y)^2}{8L} + \frac{(M_x+Pe_y)(4e_y^3-3L^2e_y+L^3)}{2L^3}$. Now, if the axis “ $x'_2-x'_2$ ” in the center of the column is located, $y_2 = e_y$ is substituted into Equation (18) and the moment is $M_{c_1/2} = \frac{P(L+2e_y)^2}{8L} + \frac{(M_x+Pe_y)(4e_y^3-3L^2e_y+L^3)}{2L^3}$. If it obtains the difference from the last equation and subtracts the first, the moment is found $M = Pe_y$. This value is exactly the moment that influences when the axial load is included.
 - c) If the axis “ $x'_2-x'_2$ ” at the free end of the footing is located, then $y_2 = -L/2$ is substituted into Equation (18) and the moment is $M = 0$.
 - d) If the axis “ $y'_1-y'_1$ ” at the free end of the footing is located, then $x_1 = L/2$ is substituted into Equation (26) and the moment is $M = 0$.
 - e) If the axis “ $y'_1-y'_1$ ” in the center of the column is located, $x_1 = e_x$ is substituted into Equation (26) and the moment is $M_{c_2/2} = \frac{P(L-2e_x)^2}{8L} + \frac{(M_y+Pe_x)(4e_x^3-3L^2e_x+L^3)}{2L^3}$. Now, if the axis “ $y'_2-y'_2$ ” in the center of the column is located, $x_2 = e_x$ is substituted into Equation (35) and the moment is $M_{c_2/2} = \frac{P(L+2e_x)^2}{8L} + \frac{(M_y+Pe_x)(4e_x^3-3L^2e_x+L^3)}{2L^3}$. If it obtains the difference from the last equation and subtracts the first, the

moment is found $M = Pe_x$. This value is exactly the moment that influences when the axial load is included.

- f) If the axis “ y'_2 - y'_2 ” at the free end of the footing is located, then $x_2 = -L/2$ is substituted into Equation (35) and the moment is $M = 0$.
- To bending shear
 - a) If the axis “ x'_1 - x'_1 ” at the free end of the footing is located, then $y_1 = L/2$ is substituted into Equation (4) and the shear force is $V = 0$.
 - b) If the axis “ x'_1 - x'_1 ” in the center of the column is located, $y_1 = e_y$ is substituted into Equation (4) and the shear force is $V_{c1/2} = \frac{P(2e_y-L)}{2L} + \frac{3(M_x+Pe_y)(4e_y^2-L^2)}{2L^3}$. Now, if the axis “ x'_2 - x'_2 ” in the center of the column is located, and $y_2 = e_y$ is substituted into Equation (13) and the shear force is $V_{c1/2} = \frac{P(2e_y+L)}{2L} + \frac{3(M_x+Pe_y)(4e_y^2-L^2)}{2L^3}$. If it obtains the difference from the last equation and subtracts the first, the shear force is found $V = P$. This value is exactly the shear force that influences when the axial load is included.
 - c) If the axis “ x'_2 - x'_2 ” at the free end of the footing is located, then $y_2 = -L/2$ is substituted into Equation (13) and the shear force is $V = 0$.
 - d) If the axis “ y'_1 - y'_1 ” at the free end of the footing is located, then $x_1 = L/2$ is substituted into Equation (21) and the shear force is $V = 0$.
 - e) If the axis “ y'_1 - y'_1 ” in the center of the column is located, $x_1 = e_x$ is substituted into Equation (21) and the shear force is $V_{c2/2} = \frac{P(2e_x-L)}{2L} + \frac{3(M_y+Pe_x)(4e_x^2-L^2)}{2L^3}$. Now, if the axis “ y'_2 - y'_2 ” in the center of the column is located, $x_2 = e_x$ is substituted into Equation (30) and the shear force is $V_{c2/2} = \frac{P(2e_x+L)}{2L} + \frac{3(M_y+Pe_x)(4e_x^2-L^2)}{2L^3}$. If it obtains the difference from the last equation and subtracts the first, the shear force is found $V = P$. This value is exactly the shear force that influences when the axial load is included.
 - f) If the axis “ x'_2 - x'_2 ” at the free end of the footing is located, then $y_2 = -L/2$ is substituted into Equation (30) and the shear force is $V = 0$.
 - To punching shear
 - a) If now the punching shear acting on the footing “ V_p ” is obtained by integration of the pressure volume of the area formed by the points 1, 2, 3 and 4 (total area) subtracting the pressure volume of the area formed by the points 5, 6, 7 and 8 (general case), then the punching shear for the general case is $V_p = P - \frac{[PL^2+12e_y(M_x+Pe_y)+12e_x(M_y+Pe_x)](c_1+d)(c_2+d)}{L^4}$. This value is exactly the punching shear that appears in Equation (42).

5. Numerical Examples. Three types of designs for square isolated footings supporting one square column of 40×40 cm are presented as in Figure 2. Dimensions of the square footings are obtained from the optimization techniques [23]. Thickness of the footing is developed as follows: the first proposal is the minimum thickness of 25 cm marked by the code of the ACI, and subsequently the thickness is revised to satisfy the following conditions: moments, bending shear, and punching shear. If such conditions are not satisfied, a greater thickness is proposed until it fulfills the three conditions mentioned [14,17-21].

5.1. Concentric footing. The column is located in the gravity center of the footing and the following information is: $H = 1.5$ m; $P_D = 700$ kN; $P_L = 500$ kN; $M_{Dx} = 140$ kN-m; $M_{Lx} = 100$ kN-m; $M_{Dy} = 120$ kN-m; $M_{Ly} = 80$ kN-m; $e_x = 0$; $e_y = 0$; $f'_c = 21$ MPa; $f'_y = 420$ MPa; $q_a = 220$ kN/m²; $\gamma_{ppz} = 24$ kN/m³; $\gamma_{pps} = 15$ kN/m³, where H is the depth of the footing, P_D is the dead load, P_L is the live load, M_{Dx} is the moment around

the axis “X-X” of the dead load, M_{Lx} is the moment around the axis “X-X” of the live load, M_{Dy} is the moment around the axis “Y-Y” of the dead load, M_{Ly} is the moment around the axis “Y-Y” of the live load, q_a is the allowable load capacity of the soil, γ_{ppz} is the self-weight of the footing, and γ_{pps} is the self-weight of soil fill. Load and moments acting on soil are: $P = 1200$ kN; $M_x = 240$ kN-m; $M_y = 200$ kN-m. Thickness of the footing that fulfills the three conditions listed above is 50 cm (effective depth is 42 cm, and coating is 8 cm) for new model and for classical model is 65 cm (effective depth is 57 cm, and coating is 8 cm), and the available load capacity of the soil “ σ_{adm} ” is 193.00 kN/m² (new model) and 191.65 kN/m² (classical model) [5,6,14,17-21]. Dimension that meets the above conditions is: $L = 3.25$ m. Pressures generated by the loads and moments at each corner are: $\sigma_1 = 190.51$ kN/m², $\sigma_2 = 120.60$ kN/m², $\sigma_3 = 106.62$ kN/m², $\sigma_4 = 36.70$ kN/m². Mechanical elements (P, M_x, M_y) acting on the footing are factored: $P_u = 1640$ kN, $M_{ux} = 328$ kN-m, $M_{uy} = 272$ kN-m. Maximum pressure for the design by classical model is: $\sigma_{max} = 260.14$ kN/m².

Substitute these values into the corresponding equations to obtain the moment, bending shear and punching shear acting in each section on the footing for the new model and classical model.

Table 1 shows the differences between the two models and Figure 6 presents the concrete dimensions and reinforcement steel of the two footings.

5.2. Edge footing. The column is located on a property line (at the end of the axis “X-X”) and the following information is: $H = 1.5$ m; $P_D = 250$ kN; $P_L = 150$ kN; $M_{Dx} = 75$ kN-m; $M_{Lx} = 50$ kN-m; $M_{Dy} = -180$ kN-m; $M_{Ly} = -120$ kN-m; $e_x = L/2 - c_2/2$; $e_y = 0$; $f'_c = 21$ MPa; $f_y = 420$ MPa; $q_a = 250$ kN/m²; $\gamma_{ppz} = 24$ kN/m³; $\gamma_{pps} = 15$ kN/m³. Load and moments acting on soil are: $P = 400$ kN; $M_x = 125$ kN-m; $M_y = -300$ kN-m. Thickness of the footing that fulfills the three conditions listed above is 40 cm (effective depth is 32 cm, and coating is 8 cm) for new model and for classical model is 55 cm (effective depth is 47 cm, and coating is 8 cm), the available load capacity of the soil “ σ_{adm} ” is 223.90 kN/m² (new model) and 222.55 kN/m² (classical model) [5,6,14,17-21]. Dimension that meets the above conditions is: $L = 1.90$ m. Pressures generated by the loads and moments at each corner are: $\sigma_1 = 220.15$ kN/m², $\sigma_2 = 220.15$ kN/m², $\sigma_3 = 1.46$ kN/m², $\sigma_4 = 1.46$ kN/m². Mechanical elements (P, M_x, M_y) acting on the footing are factored: $P_u = 540$ kN, $M_{ux} = 170$ kN-m, $M_{uy} = -408$ kN-m.

Maximum pressure for the design by classical model is: $\sigma_{max} = 306.17$ kN/m².

Substitute these values into the corresponding equations to obtain the moment, bending shear and punching shear acting in each section on the footing for the new model and classical model.

Table 2 shows the differences between the two models and Figure 7 presents the concrete dimensions and reinforcement steel of the two footings.

5.3. Corner footing. The column is located on two property lines and the following information is: $H = 1.5$ m; $P_D = 250$ kN; $P_L = 150$ kN; $M_{Dx} = -100$ kN-m; $M_{Lx} = -75$ kN-m; $M_{Dy} = -180$ kN-m; $M_{Ly} = -120$ kN-m; $e_x = L/2 - c_2/2$; $e_y = L/2 - c_1/2$; $f'_c = 21$ MPa; $f_y = 420$ MPa; $q_a = 250$ kN/m²; $\gamma_{ppz} = 24$ kN/m³; $\gamma_{pps} = 15$ kN/m³. Load and moments acting on soil are: $P = 400$ kN; $M_x = -175$ kN-m; $M_y = -300$ kN-m. Thickness of the footing that fulfills the three conditions listed above is 40 cm (effective depth is 32 cm, and coating is 8 cm) for new model and for classical model is 65 cm (effective depth is 57 cm, and coating is 8 cm), the available load capacity of the soil “ σ_{adm} ” is 223.90 kN/m² (new model) and 221.65 kN/m² (classical model) [5,6,14,17-21]. Dimension that meets the above conditions is: $L = 1.90$ m. Pressures generated by the loads and moments at each corner are: $\sigma_1 = 220.15$ kN/m², $\sigma_2 = 1.46$ kN/m²,

$\sigma_3 = 220.15 \text{ kN/m}^2$, $\sigma_4 = 1.46 \text{ kN/m}^2$. Mechanical elements (P, M_x, M_y) acting on the footing are factored: $P_u = 540 \text{ kN}$, $M_{ux} = -240 \text{ kN-m}$, $M_{uy} = -408 \text{ kN-m}$. Maximum pressure for the design by classical model is: $\sigma_{\max} = 296.54 \text{ kN/m}^2$.

Substitute these values into the corresponding equations to obtain the moment, bending shear and punching shear acting in each section on the footing for the new model and classical model.

Table 3 shows the differences between the two models and Figure 8 presents the concrete dimensions and reinforcement steel of the two footings.

Tables 1, 2 and 3, and Figures 6, 7 and 8 are shown in the Appendix.

6. Results and Discussion. Effects that govern the design for isolated footings are the moments, bending shear, and punching shear.

- For the concentric footing:
 - a) For the moment acting around the axis a_1-a_1 , there is an increase of 33% in the classical model with respect to the new model. For the moment acting around the axis a_2-a_2 , the classical model is 2.27 times greater than the new model. For the moment acting around the axis b_1-b_1 , there is an increase of 38% in the classical model with respect to the new model. For the moment acting around the axis b_2-b_2 , the classical model is 2.14 times greater than the new model.
 - b) For the bending shear acting on the axis f_1-f_1 , there is an increase of 14% in the classical model with respect to the new model. For the bending shear acting on the axis f_2-f_2 , the classical model is 1.91 times greater than the new model. For the bending shear acting on the axis g_1-g_1 , there is an increase of 18% in the classical model with respect to the new model. For the bending shear acting on the axis g_2-g_2 , the classical model is 1.81 times greater than the new model.
 - c) For the acting punching shear it presents an increase of 63% in the classical model with respect to the new model.
- For the edge footing:
 - a) For the moment acting around the axis a_1-a_1 , there is an increase of 16% in the classical model with respect to the new model. The moment acting around the axis a_2-a_2 , the classical model is 7.52 times greater than the new model. The moment acting around the axis b_1-b_1 is zero, because the column is located in the edge of the footing. For the moment acting around the axis b_2-b_2 , the classical model is 2.00 times greater than the new model.
 - b) For the bending shear acting on the axis f_1-f_1 , the classical model is 0.87 times with respect to the new model. For the bending shear acting on the axis f_2-f_2 , the classical model is 6.81 times greater than the new model. The bending shear acting on the axis g_1-g_1 is zero, because the column is located in the edge of the footing. For the bending shear acting on the axis g_2-g_2 , there is an increase of 74% in the classical model with respect to the new model.
 - c) For the acting punching shear it presents an increase of 92% in the classical model with respect to the new model.
- For the corner footing:
 - a) For the moment acting around the axis a_2-a_2 , the classical model is 3.65 times greater than the new model. For the moment acting around the axis b_2-b_2 , there is an increase of 97% in the classical model with respect to the new model. The moments acting around of the axes a_1-a_1 and b_1-b_1 are zero, because the column is located in the corner of the footing.
 - b) For the bending shear acting on the axis f_2-f_2 , the classical model is 2.46 times greater than the new model. For the bending shear acting on the axis g_2-g_2 , there

is an increase of 55% in the classical model with respect to the new model. The bending shear acting on the axes f_1-f_1 and g_1-g_1 are zero, because the column is located in the corner of the footing.

- c) For the acting punching shear it presents an increase of 2.42 times in the classical model with respect to the new model.

Materials used for the construction of the isolated footings are the reinforcement steel and concrete.

- For the concentric footing:
 - a) For the concrete, there is a saving of the 30% in the new model with respect to the classical model, because the thickness for the new model is of 50 cm and for the classical model is of 65 cm.
 - b) For reinforcement steel in direction of the axes “Y” and “X” of the footing being the same, there is a saving of the 35.73% in the new model with respect to the classical model, because the reinforcement steel in both directions for the new model is of 45.45 cm² and for the classical model is of 61.69 cm².
- For the edge footing:
 - a) For the concrete, there is a saving of 37.5% in the new model with respect to the classical model, because the thickness for the new model is of 40 cm and for the classical model is of 55cm.
 - b) For reinforcement steel in the direction of axis “Y” of the footing, there is a saving of 46.86% in the new model with respect to the classical model, because the new model is of 20.25 cm² and for the classical model is of 29.74 cm², and in the direction of axis “X” of the footing, also there is a saving of 35.23% in the new model with respect to the classical model, because the new model is of 28.19 cm² and for the classical model is of 38.12 cm².
- For the corner footing:
 - a) For the concrete, there is a saving of 62.5% in the new model with respect to the classical model, because the thickness for the new model is of 40 cm and for the classical model is of 65 cm.
 - b) For reinforcement steel in the direction of axis “Y” of the footing, there is a saving of 78.07% in the new model with respect to the classical model, because the new model is of 20.25 cm² and for the classical model is of 36.06 cm², and in the direction of axis “X” of the footing, also there is a saving of 27.92% in the new model with respect to the classical model, and with respect to the volume of reinforcement steel, because the new model is of 28.19 cm² and for the classical model is of 36.06 cm².

7. Conclusions. New model presented in this paper applies only for design of the square isolated footings with a column localized anywhere of the footing, the structural member assumes that should be rigid and the supporting soil layers elastic, which comply with the equation of the biaxial bending, i.e., the pressure variation is linear.

This paper is concluded as the following.

- 1) The new model in this paper is valid, because the equilibrium of the moments and the loads acting on the footing against the pressure exerted by the soil on the footing is verified.
- 2) The new model is adjusted to real conditions with respect to the classical model, because the new model takes account of the soil real pressure and the classical model considers the maximum pressure in all the contact surface.
- 3) The new model for design of foundations subject to axial load and moments in two directions considers one or two property lines restricted.

4) The thicknesses for the new model of the square isolated footings are governed by: for the concentric footing is the punching shear, for the edge footing is the bending shear, and for the corner footing is the punching and bending shear.

The results show that the classical model is larger than the new model in terms of the reinforcement steel and thickness of the footing. Therefore, the new model is the plus appropriate, because it is more adjusted to the real conditions of soil and also is more economic.

New model presented in this paper for the structural design of the square isolated footings subjected to an axial load and moment in two directions with a column localized anywhere of the footing, also it can be applied to other cases: 1) the footings subjected to a axial load due to the column, 2) the footings subjected to an axial load and moment in one direction due to the column.

Suggestions for future research are that when it is presents another type of soil, by example in totally cohesive soils (clay soils) and totally granular soils (sandy soils), the pressure diagram is not linear and should be treated differently.

REFERENCES

- [1] J. E. Bowles, *Foundation Analysis and Design*, McGraw-Hill, 2001.
- [2] B. M. Das, E. S. Zabay and R. A. Juárez, *Principios de Ingeniería de Cimentaciones*, Cengage Learning Latín América, 2006.
- [3] J. Calabera-Ruiz, *Cálculo de Estructuras de Cimentación*, Intemac Ediciones, 2000.
- [4] M. J. Tomlinson, *Cimentaciones, Diseño y Construcción*, Trillas, 2008.
- [5] J. C. McCormac and R. H. Brown, *Design of Reinforced Concrete*, John Wiley & Sons, Inc, 2013.
- [6] O. M. González-Cuevas and F. Robles-Fernández-Villegas, *Aspectos Fundamentales del Concreto Reforzado*, Limusa, 2005.
- [7] N. P. Kurian, *Design of Foundation Systems*, Alpha Science Int'l Ltd., 2005.
- [8] B. C. Punmia, A. K. Jain and A. K. Jain, *Limit State Design of Reinforced Concrete*, Laxmi Publications (P) Limited, 2007.
- [9] P. C. Varghese, *Design of Reinforced Concrete Foundations*, PHI Learning Pvt. Ltd., 2009.
- [10] J. H. Yin, Comparative modeling study of reinforced beam on elastic foundation, *Journal of Geotechnical and Geoenvironmental Engineering*, vol.126, no.3, pp.265-271, 2000.
- [11] J. P. Smith-Pardo, Performance-based framework for soil-structure systems using simplified rocking foundation models, *Structural Engineering Mechanics*, vol.40, no.6, pp.763-782, 2011.
- [12] R. Agrawal and M. S. Hora, Nonlinear interaction behaviour of infilled frame-isolated footings-soil system subjected to seismic loading, *Structural Engineering Mechanics*, vol.44, no.1, pp.85-107, 2012.
- [13] P. Maheshwari and S. Khatri, Influence of inclusion of geosynthetic layer on response of combined footings on stone column reinforced earth beds, *Geomechanics and Engineering*, vol.4, no.4, pp.263-279, 2012.
- [14] A. Luévanos Rojas, J. G. Faudoa Herrera, R. A. Andrade Vallejo and M. A. Cano Álvarez, Design of isolated footings of rectangular form using a new model, *International Journal of Innovative Computing, Information and Control*, vol.9, no.10, pp.4001-4021, 2013.
- [15] M. S. Dixit and K. A. Patil, Experimental estimate of $N\gamma$ values and corresponding settlements for square footings on finite layer of sand, *Geomechanics and Engineering*, vol.5, no.4, pp.363-377, 2013.
- [16] E. Cure, E. Sadoglu, E. Turker and B. A. Uzuner, Decrease trends of ultimate loads of eccentrically loaded model strip footings close to a slope, *Geomechanics and Engineering*, vol.6, no.5, pp.469-485, 2014.
- [17] A. Luévanos Rojas, Design of isolated footings of circular form using a new model, *Structural Engineering Mechanics*, vol.52, no.4, pp.767-786, 2014.
- [18] A. Luévanos Rojas, Design of boundary combined footings of rectangular shape using a new model, *Dyna*, vol.81, no.188, pp.199-208, 2014.
- [19] A. Luévanos Rojas, Design of boundary combined footings of trapezoidal form using a new model, *Structural Engineering Mechanics*, vol.56, no.5, pp.745-765, 2015.
- [20] A. Luévanos Rojas, A comparative study for the design of rectangular and circular isolated footings using new models, *Dyna*, vol.83, no.196, pp.149-158, 2016.

[21] A. Luévanos Rojas, A new model for design of boundary rectangular combined footings with two opposite sides constrained, *Alconpat*, vol.6, no.2, pp.89-104, 2016.

[22] ACI 318S-14 (American Concrete Institute), *Building Code Requirements for Structural Concrete and Commentary*, Committee 318, 2014.

[23] S. López Chavarría, A. Luévanos Rojas and M. Medina Elizondo, A mathematical model for dimensioning of square isolated footings using optimization techniques: General case, *International Journal of Innovative Computing, Information and Control*, vol.13, no.1, pp.67-74, 2017.

[24] J. M. Gere and B. J. Goodno, *Mecánica de Materiales*, Cengage Learning, 2009.

Appendix.

TABLE 1. Comparison of results for the concentric footing

Concept	New model NM	Classical model CM	CM/NM
Moment $M_{a_1-a_1}$ (kN-m)	646.22	858.39	1.33
Moment $M_{a_2-a_2}$ (kN-m)	378.47	858.39	2.27
Moment $M_{b_1-b_1}$ (kN-m)	623.36	858.39	1.38
Moment $M_{b_2-b_2}$ (kN-m)	401.32	858.39	2.14
Effective depth d (cm)	42	57	1.36
Coating r (cm)	8	8	1.00
Total thickness t (cm)	50	65	1.30
Volume of concrete (m ³)	5.28	6.87	1.30
Bending shear acting V_{f_1} (kN)	636.49	722.85	1.14
Bending shear acting V_{f_2} (kN)	377.79	722.85	1.91
Bending shear acting V_{g_1} (kN)	614.40	722.85	1.18
Bending shear acting V_{g_2} (kN)	399.87	722.85	1.81
Bending shear admissible V_f (kN)	903.88	1226.69	1.36
Punching shear acting V_p (kN)	1535.60	2502.93	1.63
Punching shear admissible V_p (kN)	2736.67	4393.45	1.61
Punching shear admissible V_p (kN)	3171.97	5631.64	1.78
Punching shear admissible V_p (kN)	1770.78	2842.82	1.61
Reinforcement steel in direction of axis "Y" A_s (cm ²)	45.45	61.69	1.36
Reinforcement steel in direction of axis "X" A_s (cm ²)	45.45	61.69	1.36

TABLE 2. Comparison of results for the edge footing

Concept	New model NM	Classical model CM	CM/NM
Moment $M_{a_1-a_1}$ (kN-m)	138.49	160.80	1.16
Moment $M_{a_2-a_2}$ (kN-m)	21.38	160.80	7.52
Moment $M_{b_1-b_1}$ (kN-m)	0.0	0.0	—
Moment $M_{b_2-b_2}$ (kN-m)	322.39	643.22	2.00
Effective depth d (cm)	32	47	1.47
Coating r (cm)	8	8	1.00
Total thickness t (cm)	40	55	1.38
Volume of concrete (m ³)	1.44	1.99	1.38
Bending shear acting V_{f_1} (kN)	216.21	191.97	0.87
Bending shear acting V_{f_2} (kN)	28.21	191.97	6.81
Bending shear acting V_{g_1} (kN)	0.0	0.0	—
Bending shear acting V_{g_2} (kN)	337.60	588.90	1.74
Bending shear admissible V_f (kN)	402.61	591.33	1.47
Punching shear acting V_p (kN)	480.43	920.08	1.92
Punching shear admissible V_p (kN)	1169.68	1998.07	1.71
Punching shear admissible V_p (kN)	1373.90	2701.69	1.97
Punching shear admissible V_p (kN)	756.85	1111.62	1.47
Reinforcement steel in direction of axis “Y” A_s (cm ²)	20.25	29.74	1.47
Reinforcement steel in direction of axis “X” A_s (cm ²)	28.19	38.12	1.35

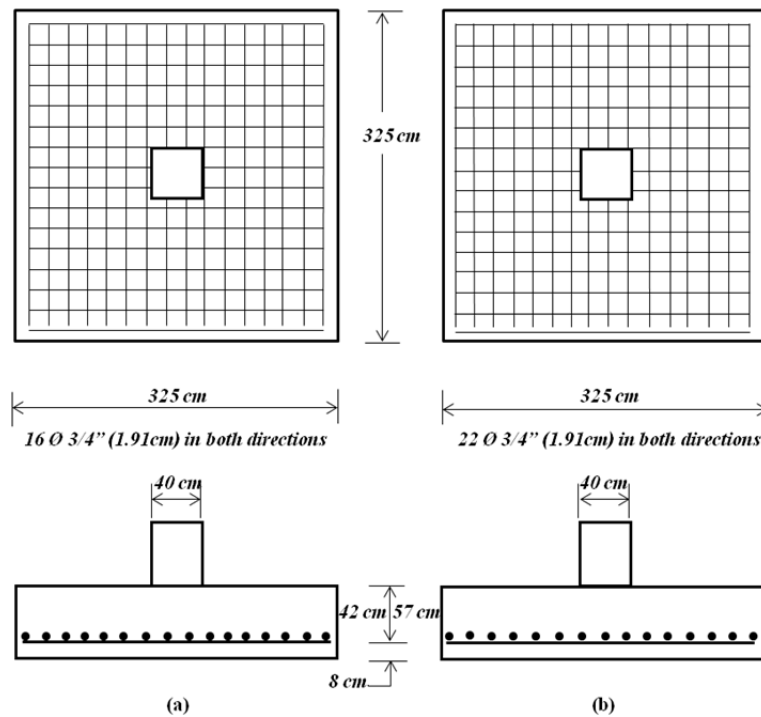


FIGURE 6. Concentric footing: (a) new model, (b) classical model

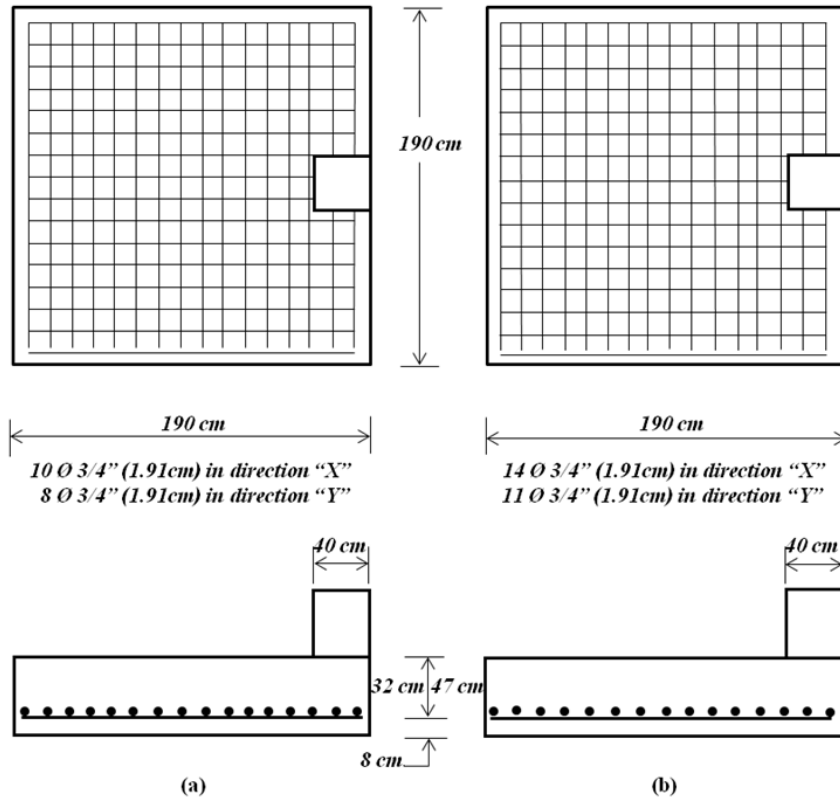


FIGURE 7. Edge footing: (a) new model, (b) classical model

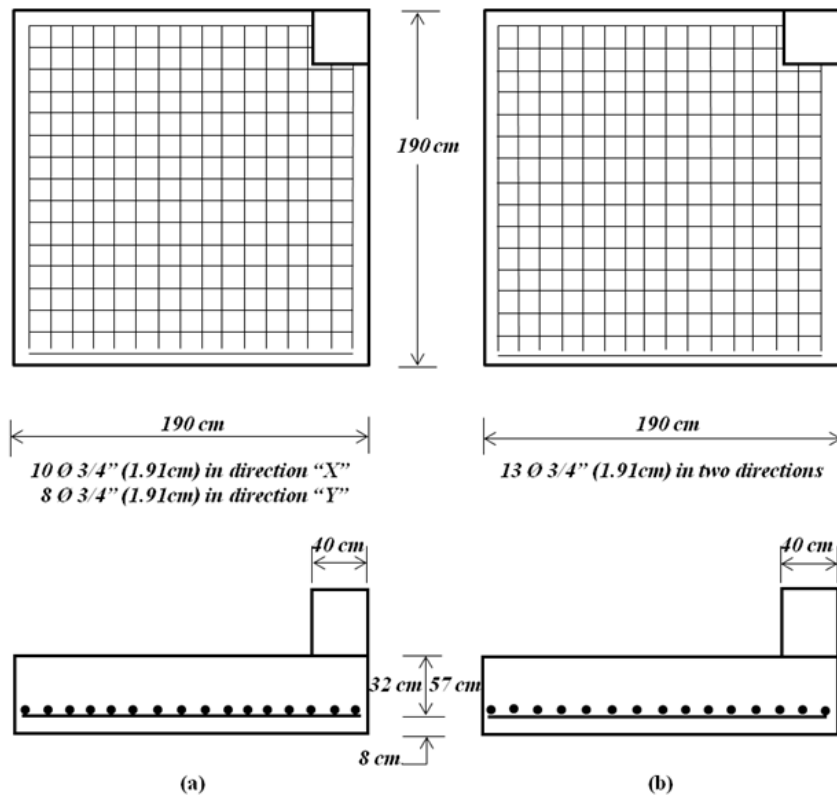


FIGURE 8. Corner footing: (a) new model, (b) classical model

TABLE 3. Comparison of results for the corner footing

Concept	New model NM	Classical model CM	CM/NM
Moment $M_{a_1-a_1}$ (kN-m)	0.0	0.0	—
Moment $M_{a_2-a_2}$ (kN-m)	173.60	633.85	3.65
Moment $M_{b_1-b_1}$ (kN-m)	0.0	0.0	—
Moment $M_{b_2-b_2}$ (kN-m)	322.39	633.85	1.97
Effective depth d (cm)	32	57	1.78
Coating r (cm)	8	8	1.00
Total thickness t (cm)	40	65	1.63
Volume of concrete (m ³)	1.44	2.35	1.63
Bending shear acting V_{f_1} (kN)	0.0	0.0	—
Bending shear acting V_{f_2} (kN)	212.74	523.99	2.46
Bending shear acting V_{g_1} (kN)	0.0	0.0	—
Bending shear acting V_{g_2} (kN)	337.60	523.99	1.55
Bending shear admissible V_f (kN)	402.61	717.14	1.78
Punching shear acting V_p (kN)	383.50	931.37	2.42
Punching shear admissible V_p (kN)	711.98	1551.29	2.18
Punching shear admissible V_p (kN)	893.86	2237.18	2.50
Punching shear admissible V_p (kN)	460.69	1003.78	2.18
Reinforcement steel in direction of axis “Y” A_s (cm ²)	20.25	36.06	1.78
Reinforcement steel in direction of axis “X” A_s (cm ²)	28.19	36.06	1.28